PATTERNED MAGNETIC THIN FILMS FOR ULTRA HIGH DENSITY RECORDING

J.C. LODDER, M.A.M. HAAST AND L. ABELMANN
Information Storage Technology Group, MESA+ Research Institute, University of Twente, 7500 AE Enschede, The Netherlands
WebPage: :www.el.utwente.nl/tdm/istg/
E-mail: j.c.lodder@el.utwente.nl

Abstract

The areal bit density of magnetic disk recording has increased since 1990 60% per year and even in the last years 100%. Extrapolation of these rates leads to recording parameters not likely to be achieved without changes in the present way of storing hard disk data. One of the possible solutions is the development of so-called patterned magnetic media. Such media will also shift the superparamagnetic limit positively in comparison with the present thin film media. Theoretically, a bit density in the order of Tbits/in^2 may be possible by using this so-called discrete magnetic recording scheme. The patterned structures presented in this paper consist of a regular two-dimensional array of single domain dots with large uniaxial magnetic anisotropy and have been prepared from CoNi/Pt multilayers with strong intergranular exchange coupling and large perpendicular magnetic anisotropy. For the preparation of the patterned media, a patterning process based on Laser Interference Lithography method (LIL) and Ion Beam Etching has been developed. This technology provides the possibility to pattern 2-D arrays of submicron dots smaller than the critical size for the transition from multi to single domain. The smallest prepared dot sizes are 60 nm with a center-to-center dot spacing of 200 nm and thickness of 30 nm. The magnetic characterization of these dots showed that they are single domain with reasonable coercivity and good thermal stability. Micromagnetic simulations show that the single domain state is the lowest energy state for dots with a diameter below 75nm, which confirms the experimental observations.

1. Introduction

The micro-technology industry, which has made incredible progress over the last decades by continuously scaling down feature sizes, is currently facing fundamental barriers. The main areas of this industry are microelectronics and data storage. In the area of microelectronics, the light diffraction limit forces industry to investigate new ways of lithography. Simultaneously, the area of data storage is facing similar barriers. Since the dimensions of written bits are decreasing much faster than the linewidth in microelectronics, these barriers are more eminent. One of the most important barriers is the thermal stability of written bits; as the bit-size gets smaller, the energy stored in the

bit becomes comparable to thermal energy fluctuations. The stability of written data with time is therefore now a major concern in hard-disk design, and is receiving wide spread attention in magnetic recording research. The areal bit density of magnetic disk recording has increased prodigiously over the last decades [1]. Extrapolation of these rates leads to bit densities not likely to be achieved without changes in the present way of storing hard-disk data. One of the solutions is the development of a so-called patterned magnetic media [2-9]. Such media will help to overcome the superparamagnetic limit of present thin film media, which is expected to be at around 100 Gbit/in^2. Although the data-density in hard disks has doubled every 15 months during the last decade, the access time only decreases with 7% per year [3]. Studies by Intel [10] have shown that this discrepancy will lead to a loss in the performance of desktop computers. If the access times are not seriously improved, this loss will be 60% in 2003. After that the added value of a processor with higher clock-speed will become minimal. This is, as one can understand, a major worry for the semiconductor industry, but also for the storage industry. The reason for this slow decrease in access time lies in the hard-disk architecture. The access time is mainly determined by the time it takes for the disk to rotate to the desired location. The underlying, fundamental, problem is that the hard-disk architecture does not scale well. There is only one head per side of the disk, so the ratio between the number of heads and the number of bits in the disk is rapidly decreasing with increasing capacity. Ideally, for a well scalable architecture, this ratio should be independent of capacity. The solution to the access time problem is therefore to radically change the hard disk architecture so that it becomes scalable. If one sticks to mechanical addressing, the only solution is to increase the number of heads. Since thousands of heads are needed, future systems will require micro-mechanical designs, such as the IBM Millipede [11]. In this system, which is might be called a scanning probe array recording system, a 32x32 array of micro-mechanical read/write heads is scanned in a rectangular fashion over a recording medium. In principle such a system can be based on optical, mechanical, thermal and magnetic detection principles. Theoretically a bit density in the order of Tbits/in^2 may be possible by using the discrete magnetic recording scheme. Patterned media can be made by various techniques such as e-beam lithography, ion implantation and Laser Interference Lithography (LIL). The latter will be discussed in this paper for preparing a patterned magnetic medium. Such a medium should consist of a regular two-dimensional array of single domain dots with large uniaxial magnetic anisotropy. This technology provides the possibility to pattern 2-D arrays of magnetic dots smaller than the critical size for the transition from multi to single domain.

1.1. REQUIREMENTS FOR PATTERNED MEDIA

The principle of patterned media has already been proposed in the 60's to overcome problems associated with head positioning on the track [12]. The magnetic material for these media was thought not to be different from that of the continuous (thin film) media. Recently, it was proposed that patterned medium recording with a '1 dot = 1 bit' principle would give additional advantages if the dots would be single domain [13, 14]. Then the constraints on the writing and reading process itself are strongly reduced. Due to the single domain nature of every dot, the writing of such a bit is an all-or-nothing event and the head does not have to be positioned exactly above the bit. Besides, the

signal to noise ratio of the read-back signal is much better due to the absence of media noise and transition shifts. Moreover, the superparamagnetic bit density limit of this type of medium is much higher than that of present thin film media. For the design of a prototype patterned medium for recording several requirements can be given:

1. The dots should be in a regular 2D matrix having a low amount of defects
2. High uniaxial anisotropy so that they are single domain and thermal stable.
3. Narrow switching field distribution (by realizing an uniform size and shape) and a small dipolar interaction.
4. The number of 'bad bits' due to missing dots or inhomogeneities in the magnetic material should be small.

2. Submicron patterning technologies

For a successful application of the concept of patterned media recording the development of a suitable patterning technique is one of the crucial items. The requirement of patterning large areas of regularly spaced uniform dots at nano-dimensions puts strong demands on the patterning technology. Even in the R&D lab such technologies are generally not readily available, not to speak of manufacturing. However, in this contribution the goal is not to design a patterning technology for the manufacturing of a patterned disk but to discuss a prototype of a patterned medium and study its relevant magnetic properties. Three types of patterning technologies will be distinguished. Two are lithographic techniques based on the patterning of resist layers, either with or without a pre-patterned mask. Only the step of pattern generation is discussed here. In general, this pattern has to be transferred to a magnetic layer by common techniques such as lift-off, etching or electrodeposition. Each of these post-lithography steps is also encountered in section 3 where complete processes based on laser interference lithography are discussed. Another type is the family of resist-less patterning techniques which are either single- or two-step patterning processes.

2.1. NANO-PATTERNING WITH A PRE-PATTERNED MASK

In state of the art of production of integrated circuits minimum feature sizes are already below 180 nm and these critical dimensions are still decreasing. For the production of these devices optical lithography based on wafer steppers is used. These steppers are equipped with an excimer laser and demagnify structures on a patterned mask on the substrate wafer. The decrease of the feature size is mainly made possible by the application of lasers with shorter wavelength. At present 248 nm KrF lasers are used in IC production and processes with 193 nm ArF laser are under development [15]. However, it is generally realized that for sub-100 nm devices a new generation of lithography techniques needs to be developed [16]. Among the candidates are proximity x-ray – [17], extreme ultra-violet – [18], electron projection – [19] and ion projection lithography [20]. All these technologies require big and expensive machines and might not be suitable for the production of patterned media. However, for R&D purposes they are very interesting. For instance, Rousseaux et al. have successfully patterned high quality submicron magnetic dots with minimum dot sizes of 200 nm by x-ray lithography [21]. Parallel to these developments, still much cheaper optical lithography

schemes are being proposed for the realization of sub-100 nm resolution and certainly worth mentioning here: optical lithography with light-coupling [22] or phase [23] masks and near-field optical lithography [24]. Another truly promising and emerging submicron patterning technology is nano-imprint or hot-embossing lithography 25-27]. Nanosized holes are physically printed in a thin polymer layer with a mold. With this technology Kong et al. have demonstrated the preparation and writing of a patterned medium of 10 Gbit/in^2 [28]. Despite of the reported results the technology is still under development and several problems, amongst others the adhesion between mold and substrate, need to be solved [29]. A technology related to nano-imprint lithography is microcontact printing with self-assembled monolayer (SAM) resists [27,30]. A pattern of SAM can directly be 'deposited' by printing with a stamp and does not even require the large forces needed with nano-imprint. Alternatively, the self-assembling capacity of polymers may be used to form a dot pattern without a stamp [31]. However, the limits of the latter technique still need to be explored.

2.2. NANO-PATTERNING WITHOUT RESIST LAYERS

Instead of using resist layers for pattern definition, the desired pattern may also be directly written in the magnetic layer or even be directly deposited. Examples of direct writing are demonstrated by Allenspach *et al.* and Aign *et al.*, who have patterned magnetic layers with a focussed electron beam [32] and with a focussed ion beam [33] respectively. In both cases the magnetic anisotropy of the magnetic material has locally been modified by electron bombardment respectively ion irradiation. Though these techniques only allow the patterning of small areas, especially the focussed ion beam technology seems very promising for basic studies on patterned media. As Aign *et al.* have shown, minimum dot separations of only 20 nm can be obtained, which allowed studies of dipolar interactions in patterned media. The ideal way of the preparation of a patterned medium is the direct deposition of dots. Three such techniques are briefly discussed here: sequential deposition of islands, self-organization and laser-focussed atomic deposition. Though restricted to small areas, scanning probe microscope and again focussed ion beam technology can deposit submicron islands in a sequential way. An example is the work of Bessho *et al.*, who deposited a variety of nanosized magnetic dots with a commercial atomic force and scanning tunneling microscope [34]. Direct deposition of nanosized islands over large areas is attracting much interest for electronic applications of quantum dot arrays. These dots are formed by a process of self-organization during the deposition of multilayers of semiconductors [35] and can be used as templates for a patterned medium. Using self-organized $Si_{1-x}Ge_x$ films and shadow deposition of Co, Teichert *et al.* have shown the preparation of reasonably regular arrays of 25 x 35 nm^2 Co islands [36]. The major drawback of this type of patterning is the complexity of the growth of the self-organized pattern. Finally, an alternative to self-organization of semiconductors is the direct deposition with neutral atom lithography. As with laser interference lithography an interference pattern of two laser beams is used for pattern definition. Instead of exposing a resist layer, the line or dot pattern is directly deposited by the effect of laser-focussed atom deposition. With this technique Celotta *et al.* have demonstrated the preparation of 80 nm Cr dots [37]. Though, at present, this technology works only for a limited number of materials, Cr dots may be used as an etching mask for preparing magnetic dots. Another interesting

option is the use of the laser-focussed atoms for the exposure and etching of a self-assembled monolayer resist [38] or the growt of a carbonaceous resist [39]. Recently, atomic beam holography has been proposed as further expansion of neutral atom lithography [40]. A resolution of several nanometers would be possible with this technique.

2.3. NANO-PATTERNING WITHOUT A MASK

For the preparation of limited numbers of nanosized devices electron beam lithography (EBL) is more or less the standard patterning technology. The principle of the technique is the direct writing of the desired structures in a thin resist layer (PMMA) with a focussed electron beam. The resolution is well below 100 nm. Recently the preparation of metallic dot arrays with 25 nm period was reported [41]. This implies that the preparation of a patterned medium with a bit density of 1 Tbit/in^2 is in principle possible. Several groups have indeed successfully applied EBL for the preparation of magnetic dots for storage applications. The minimum dot sizes are 100 nm [42], 50 nm [43] and 20 nm [44]. However, large areas can not readily be patterned with EBL and macroscopic magnetic characterization is therefore not reported on this type of samples. Alternatively, EBL can be used for the preparation of masks, which can be used in one of the lithographic technologies described in the previous subsection. The preparation of the mold for the nano-imprint technique is such an example [25]. Besides the sequential writing of resist structures with EBL, a true optical maskless lithographic technology exists for the preparation of uniform sub-100 nm lines and dots: i.e laser interference or holographic lithography (LIL).

3. Laser Interference Lithography

Because of its simplicity, potential and availability laser interference lithography (LIL)was selected as the technology for the submicron patterning of magnetic thin films in this work. In LIL a resist layer is exposed by an interference pattern generated by two obliquely incident laser beams.

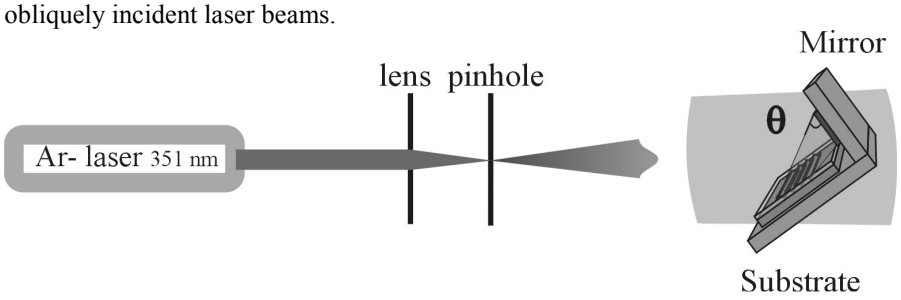

Figure 1: Setup for the pattern exposure in laser interference lithography.

The principle of the exposure with the interference pattern is shown in Figure 1. In this configuration the interference pattern is formed by a ‘direct-incident’ beam and a ‘mirror-reflected’ beam and is called the ‘mirror’ method. After development of the

resist, lines are formed. The periodicity p of the lines is determined by the wavelength λ and the angle of incidence Θ of the laser beams:

$$p = \frac{\lambda}{2\sin\Theta} \quad (1)$$

Dots can simply be fabricated by a second exposure after rotating the substrate over 90º. The patterned area is determined by the diameter of the two laser beams. For processes with no need for alignment, LIL is relatively simple and cheap and therefore the method of choice. Although this technique is not widely known, LIL is already used for more than twenty years for the preparation of submicron gratings for application in integrated optics [45,46]. In recent years the possibility of patterning large areas of dots with LIL has been recognized. Now LIL is attracting great attention for a wide variety of applications, amongst others: field emission displays [47-49], patterned magnetic media [50-53], antireflection-structures [54], photonic crystals [55], microfiltration [56] and mask-making for nanoimprint [57] and X-Ray lithography [58]. Its capability for patterning large areas is clearly demonstrated by the fabrication of 50 x 50 cm^2 areas of submicron dots [59] and allows the use of standard magnetic characterization tools on 1x1 cm^2 samples in studies on patterned media [60].

3.1. DIFFERENT APPROACHES TO LASER INTERFERENCE LITHOGRAPHY

Other research groups use a beam-splitter and two mirrors to make the interference pattern (the 'two-beam' method, see for instance [51,52,61]. For the preparation of isolated magnetic dots by LIL, several processing schemes have been developed and are based on the deposition in resist holes by electroplating [52] or evaporation-and-lift-off [50,51], or, as in this work, on the selective removal of sputter-deposited material by etching [53]. For the selection of most suitable processing scheme three criteria are important: i.e. the tailoring of the material properties, the process latitude for pattern definition and the influence of the patterning process on the final magnetic properties of the dots. The first criterion favors deposition by sputtering or perhaps evaporation. As pointed out by Fernandez *et al.* the second criterion favors a process based on resist dots rather than holes [61,62]. They have shown that using positive-tone resist the patterning of holes has inferior exposure latitude or requires complex image reversal schemes. Moreover, they state that the limited sensitivity and contrast of negative-tone resist cannot solve this problem. The third criterion encompasses effects like the damage induced by resist baking or etching on the dots' magnetic properties and the dot uniformity. From this point of view a post-patterning deposition would be favorable, though not by electroplating. In Table1 a summary of the comparison of the three processing schemes is given. To conclude this overview of possible processing schemes it should be mentioned that an interesting alternative to etching might be ion irradiation to alternate material properties without physically removing the material. Chappert *et al.* showed that the perpendicular anisotropy could be locally destroyed in Co/Pt multilayers by irradiation of resist lines with He^+ [63]. Though the resist lines were not prepared by LIL, this technique may also be incorporated in a process based on LIL.

TABLE 1: A comparison of possible processing schemes for the preparation of magnetic dots with laser interference lithography.

Process	Advantage	Disadvantage
Resist holes + electroplating	- Requires no etching and allows deposition after processing. - Most simple	- Inferior process latitude for the preparation of resist holes. - Limited to single element pillars and possible bad uniformity of pillar height.
Resist holes + lift-off	- Requires no etching and allows deposition after processing. - The material properties can be well tailored.	- Inferior process latitude for the preparation of resist holes. - Growth in resist holes may result in uncontrolled shapes. - Lift-off processes are not reliable.
Pre-deposited magnetic material + resist dots and etching	- The material properties can be well tailored. - Superior process latitude for the preparation of resist dots	- Material properties may deteriorate during processing.

3.2. DESIGNED PATTERNING PROCESS

Since the first objective was the patterning of tailored magnetic films, such as sputtered $Co_{50}Ni_{50}$/Pt multilayers, the third processing scheme in Table 1 was selected. Here the separate steps of the designed process are described. As a first step, 3" Si (100) wafers are thermally oxidized by a wet oxidation process. Usually 100 to 600 nm thick siliconoxide layers are grown to serve as a diffusion buffer between the silicon and the magnetic thin film, which is subsequently deposited. Then a thin positive-tone resist layer is spun on top of the magnetic thin film. Standard Shipley 1805 resist is used. The thin resist layers are prepared by diluting the resist with EC solvent (i.e. propylene glycolmonomethyl etheracetate) and spinning at high speed. The final thickness is determined by the ratio of the mixture and the spinning time. Measurements by ellipsometry showed that the resist layer thickness is both highly homogeneous (at the resolution of the laser spot, i.e. < mm) and very reproducible. Over a 3" wafer the thickness varies less than 1% and between different wafers the variation is a few % at most. Here it is interesting to mention that also thin resist layers with similar quality could be prepared on 1x1 cm^2 samples glued on a 3" wafer. Only in an area within 1 mm from the edge the thickness seems to deviate strongly. Apparently also small samples can be patterned with laser interference lithography. The resist is exposed with an interference pattern using the setup shown in Figure 1. By varying the angle of the substrate with the laser beam from 18° to 61° the periodicity of the interference pattern is decreased from 600 nm to 200 nm. The patterned area is inversely proportional to this angle. At 18° the area is 7x7 mm^2. For angles larger than 45° the area is limited to the size of the mirror, i.e. approximately 25x25 mm^2. In the next section the interference pattern itself will be discussed in more detail. Development of the exposed resist occurs in a diluted solution of standard developer Microposit 351 (1:7) for 5-15 s. The developed resist pattern is transferred into the magnetic layer with ion beam etching (IBE). IBE is the method of choice for this purpose, because reactive ion etching of magnetic materials is still excluded by the lack of appropriate etching recipes. Since

IBE is a purely physical etching process, the etching rates of various materials are approximately equal. This means that the thickness of the magnetic dot is roughly limited to the thickness of the resist dot.

3.3. $CO_{50}NI_{50}$/PT MULTILAYERS FOR PATTERNING

The numerous studies on Co- and CoNi-based multilayers show that, if deposited under the right conditions, these multilayers may have both a strong intergranular exchange coupling and a large perpendicular magnetic anisotropy. Therefore Co- and CoNi-based multilayers may be very suitable for application as patterned medium. In the mid-1980's Carcia *et al.* [64,65] discovered the perpendicular magnetic anisotropy in Co/Pt and Co/Pd multilayers. Due to their potential interest for magneto-optic recording these multilayers have attracted great interest and their properties have extensively been studied [66-69]. In spite of promising results the relatively high Curie temperature of Co-based multilayers remained an issue. This problem could be overcome by replacing the Co layer by a $Co_{1-x}Ni_x$-alloy layer [70-74]. The Curie temperature has considerably been reduced while other magnetic and magneto-optic properties, like the perpendicular magnetic anisotropy and polar Kerr rotation, hardly deteriorated.
It is interesting to note that the recording principle of such a medium then could be either based on magnetic probes or on magneto-optic technology. Moreover, the large polar Kerr rotation provides the possibility to benefit from sensitive characterization tools, such as Polar Kerr Magnetometry and Microscopy. Motivated by these expectations, sputtered $Co_{50}Ni_{50}$/Pt multilayers were selected as magnetic material for our research on magnetic micro- and nanostructures.

3.3.1. Deposition of CoNi/Pt multilayers

The deposition method used in this work is a plasma free magnetron sputtering. The base pressure of the system is smaller than $5 \cdot 10^{-8}$ mbar. The sputtering gas is Argon and the deposition pressure can be varied from 6 to 36 μbar. The deposition rates are kept low for a good control of layer thickness and assure a smooth layer growth. Pt is DC (30 W, V ≈ 400 V) sputtered with a typical deposition rate of 1.6 Å/s. $Co_{50}Ni_{50}$ is RF (40 W, 13.52 MHz) sputtered with a typical deposition rate of 0.5 Å/s. A more extensive description of the system can be found elsewhere [75]. The $Co_{50}Ni_{50}$/Pt multilayers for patterning consists of 26 bilayers of $Co_{50}Ni_{50}$ (6 Å) / Pt (6 Å) and is deposited at 12 μbar. In all cases we used a 6 Å Pt seedlayer between the thermally oxidized Si substrate and the multilayer stack. Such layer shows a large perpendicular magnetic anisotropy ($H_{K,eff} = (4.7 \pm 0.2) \cdot 10^2$ kA/m) and a strong intergranular exchange coupling. Therefore, the basic requirements for a patterned storage medium have been fulfilled.

3.3.2. Magnetization reversal in the optimized $Co_{50}Ni_{50}$/Pt multilayer

Both minor and major hysteresis curves of the optimized $Co_{50}Ni_{50}$/Pt multilayer are shown in Figure 2. The magnetization reversal is similar to that observed by Kooy *et al.* in thin plates of bariumferrite [76]. After saturation, the magnetization of the multilayer nucleates into a stripe domain pattern at the nucleation field H_N, in this case close to zero. With a small increase of the applied field beyond the nucleation field this stripe domain pattern becomes a demagnetized state with zero net magnetic moment. Upon further increase of the applied field the reversed domains grow at the cost of the

unreversed ones. Finally, saturation is reached at the saturation field H_S. This specific type of magnetization reversal is a good indication for the strong intergranular exchange coupling of the multilayer.

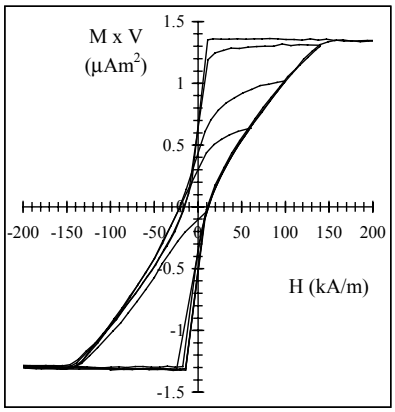

Figure 2: *Major and minor VSM hysteresis curves of the Pt (6 Å)/{$Co_{50}Ni_{50}$ (6 Å)/Pt (6 Å)} x 26 multilayer deposited at 12 μbar on a thermally oxidized silicon substrate.*

4. Important magnetic properties for small structures.

Besides the interest from the viewpoint of application, media with the above-mentioned properties are exceptionally suitable for more fundamental studies. In particular, the mechanisms of magnetization reversal and the role of the activation volume are still not well understood for experimental single domain particles. The main problem is the availability of samples of particles with a low distribution of particle size, narrow distribution of anisotropy orientation and minimal magnetostatic interactions. All these problems are not present in an above-described patterned medium. In the following sections, several issues important for studies on single domain particles/dots will be discussed.

4.1. UNIAXIAL MAGNETIC ANISOTROPY

For the realization of uniaxial magnetic anisotropy several different types of materials can be used. The origin of their magnetic anisotropy can be in their microstructure (crystal or structural anisotropy), induced by the geometry of the dot or particle (shape anisotropy) or due to a layered structure (interface anisotropy):
Crystal anisotropy. Classical examples of materials with a (large) crystal anisotropy are hcp-oriented cobalt and bariumferrite. Both materials can be deposited as (ultra) thin films with a highly oriented structure and an anisotropy constant approaching the bulk values [77,78]. Materials with an extremely high crystal anisotropy are Fe or Co based alloys with $L1_0$ phase, such as FePt, CoPt and FePd. Thin films of these materials generally have a reduced, but still very high, anisotropy constant [79-81].

Shape anisotropy. Shape anisotropy is present when a magnetic particle has a non-spherical shape and will be uniaxial.
Interface anisotropy. Interface anisotropy is assumed to be the cause of the large perpendicular anisotropy observed in Co-based multilayers with thin (< 10 Å) Co layers [82]. In these multilayers the total effective magnetic anisotropy, K_{eff}, is phenomenologically described by [83]:

$$K_{eff} \cdot t = 2 \cdot K_i + K_v \cdot t \qquad (2)$$

where K_i and K_v are the interface resp. volume anisotropy and t is the magnetic layer thickness. The volume anisotropy can consist of crystal, shape and magnetoelastic contributions. The former two have been discussed above. The latter is caused by an inhomogeneous strain in the crystal lattice of the magnetic layer. Especially, in the case of multilayers of materials with a large difference in lattice spacing the magnetoelastic anisotropy may be considerable.

TABLE 2: Bulk and experimental values of saturation magnetization, uniaxial anisotropy constant and anisotropy field for some magnetic materials.

Material	**M_s (kA/m)**	**K_u (kJ/m^3)**	**$H_{K,u}$ (kA/m)**
Co (hcp)	1420	450	500
Co (fcc)	1420	(640) [1]	(700) [1]
Ni	480	(75) [1]	(240) [1]
Fe	1700	(920) [1]	(860) [1]
$BaFe_{12}O_{19}$	350	300	1300
FePt ($L1_0$ phase) [2]	1100	4000	5700
TbFeCo [3]	100	100	1600
$Co_{50}Ni_{50}$/Pt (multilayer) [4]	500	480	1500

[1] For shape anisotropy of quasi-infinitely elongated pilars (aspect ratio >> 1).
[2] Value from [80]. For bulk CoPt and FePt, K_u = 2.8 resp. 7.0 MJ/m^3. Thin film CoPt and FePt with $L1_0$ phase usually have a considerably lower anisotropy constant.
[3] Value from [106]. TbFeCo is a ferrimagnet. Its magnetization strongly depends on the compensation temperature.
[4] This work. Due to the modulation of magnetic and non-magnetic layers its shape anisotropy is proportional to $\overline{M_s^2}$ instead of $\overline{M_s}^2$ [107].

In Table 2 an overview is given of the saturation magnetization and uniaxial anisotropy constant of the materials mentioned above. The switching field that can be expected for single domain dots patterned from these materials is strongly determined by these properties.

$$H_{K,u} \equiv \frac{2K_u}{\mu_0 M_s} \qquad (3)$$

The upper limit of the switching field (corrected for demagnetization) is given by the nucleation field of a particle, which has a magnetization reversal by coherent rotation (Stoner-Wohlfarth particle). This value is called the anisotropy field and is given by

formula (3). For all materials the calculated value, also shown in Table 2, seems more than sufficient for storage purposes.

4.2. CRITICAL DIAMETER FOR MAGNETIC DOTS.

A magnetic particle will prefer single domain if the energy of a two-domain state is larger than that of a single-domain state. For a cylindrical dot, as shown in Figure 3, this transition will occur at a critical diameter d_{crit}..

d < d crit **d > d crit**

Figuur 3: *Schematic view of single and multi domain cylinders.*

By considering only the magnetostatic and domainwall energy an estimation of the critical dot diameter d_{crit} for the transition from a single to a two domain state can be found in [9]:

$$d_{crit} \approx \frac{32}{\pi} \frac{Q \cdot \delta}{N_z(h, d_{crit})} \tag{4}$$

Here, $N_z(h,d)$ is the (average) demagnetizing factor of the cylinder, which depends on the cylinder height h and diameter d and Q is defined by:

$$Q \equiv \frac{K_u}{\frac{1}{2}\mu_0 M_s^2} \tag{5}$$

and

$$\delta \equiv \sqrt{\frac{A}{K_u}} \tag{6}$$

This expression is used in micromagnetics to represent the wall width (δ) and actually is the Landau and Lifschitz wall width [84].

5. Magnetic behaviour of submicron dots.

For all samples the standard $Co_{50}Ni_{50}$/Pt multilayer as earlier discussed has been used. At a fixed period of 570 nm, arrays with different dot diameter *D* have been prepared by varying the exposure dose in LIL. The final dot size, determined with SEM, was shown to be in the range between 140 and 280 nm: 140, 180, 280 (I) and 280 (II) nm. For all 570 nm arrays the dots have the shape of a disk and after etching a thin resist layer remains on their top (see Figure 4).

The exposure time for the 200 nm array was shown to be very critical and therefore for this study only one dot diameter was patterned.

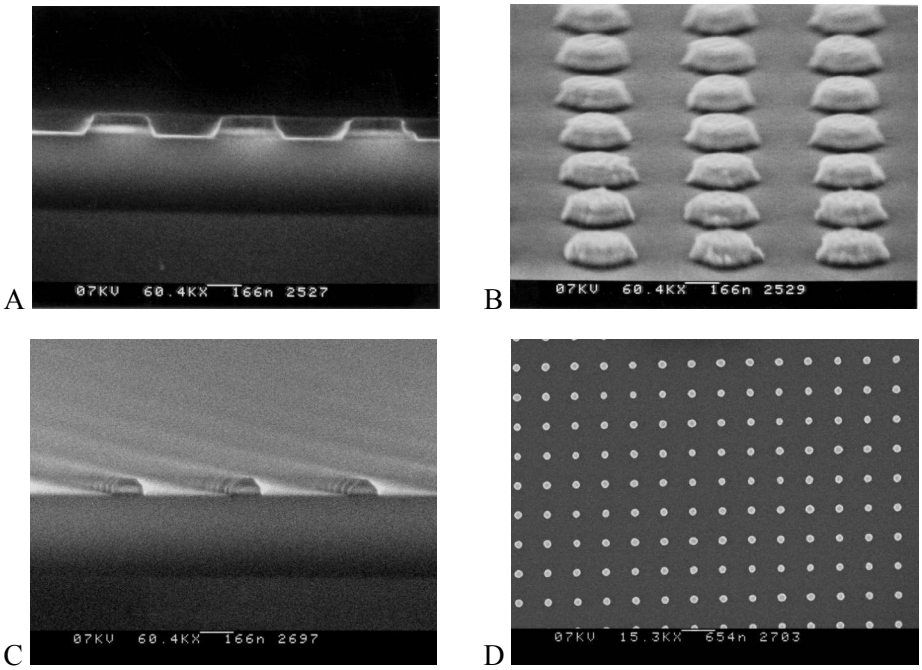

Figure 4: SEM images of submicron Co50Ni50/Pt multilayer dots prepared with Laser Interference Lithography at a fixed period of 570 nm: A) Cross section of 280 nm dots; B) Oblique view of 280 nm dots; C) Cross section of 140 nm dots; D) Top view of 140 nm dots.

These dots have the shape of a pyramid or cone (see Figure 5). After etching no resist was left on their top, which means that the multilayer has partially been etched and the total thickness has been reduced to approximately 15 nm.

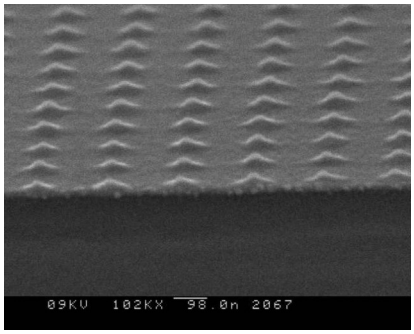

Figure 5: *SEM image of nanoscale $Co_{50}Ni_{50}$/Pt multilayer dots prepared with Laser Interference Lithography at a period of 200 nm.*

The area of the 200 nm arrays is around 2.5 x 2.5 cm^2, from which four samples were cut. Because the dot size was inhomogeneous over the whole area, *D* of each sample varied from 60 to 80 nm.

5.1. MFM OBSERVATIONS

With Magnetic Force Microscopy (using EBID tips [85]) the domain state after in-plane demagnetization of the samples with *D* = 180 nm and 70 nm has been imaged. As shown in Figure 6, the 180 nm dots are multi domain (MD) with two or three domains, while for the 70 nm dots only single domain (SD) states are observed.

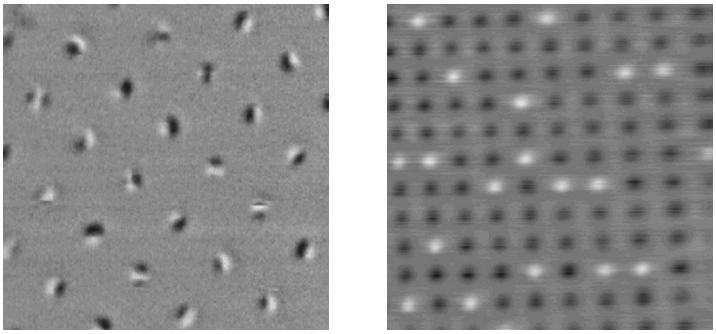

Figure 6: *Magnetic force microscopy images of $Co_{50}Ni_{50}$/Pt multilayer dots with different dot diameter: 180/570 nm and multi domain; 70/200 nm and single domain (right).*

5.2. HYSTERESIS AND INITIAL MAGNETIZATION

The perpendicular hysteresis curves of the 70 nm and 180 nm dots are shown in Figure 7. They look very similar. In fact, the hysteresis curve has an identical shape for all samples: the remanence is close to 100 % and the reversal takes place in a narrow field range around H_c. In Table 3 H_c is given as function of *D*.

TABLE 3: H_C, $H_{K,eff}$ and demagnetized domain state as function of dot size. Also the properties of the unpatterned multilayer are given.

D (nm)	**H_C (kA/m)**	**$H_{K,eff}$ (kA/m)**	***SD/MD***
60 – 80	120 - 80	500	SD
140	260	850	SD/MD
180	180	700	MD
280 (I)	160	700	MD
280 (II)	250	800	MD
$Co_{50}Ni_{50}$/Pt multilayer	15	500	MD

Over the whole range, no clear relation between D and H_c is found. This phenomenon will be discussed later. Both the initial magnetization curves and the in-plane hysteresis curves are significantly different for the 180 nm multi domain dots and 70 nm single domain dots (Figure 7). The 180 nm dots show smooth domain wall movement and the in-plane remanence is non-zero, while the 70 nm dots show switching similar to the

perpendicular hysteresis curve and the in-plane remanence is zero. Apparently, for these samples, the demagnetized domain state can be probed by both the initial magnetization and the in-plane hysteresis measurements. Therefore, initial magnetization curves have been used to determine the demagnetized domain state for all samples. The results are also shown in Table 3. The initial magnetization curve of the 140 nm dots shows both MD and SD states (see Figure 8). So the transition from SD to MD occurs somewhere inbetween 70 and 180 nm, probably close to about 140 nm, where both states co-exist.

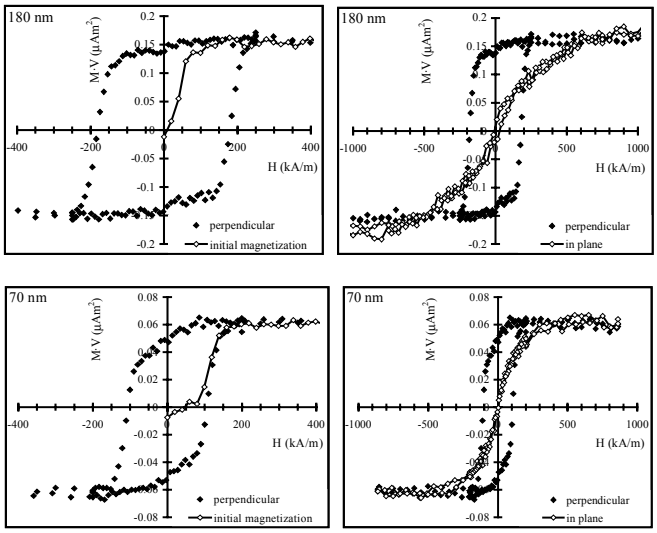

Figure 7: *VSM hysteresis and initial magnetization curves for 180/570 nm (top) and 70/200 nm (bottom) $Co_{50}Ni_{50}$/Pt multilayer dots.*

Now the demagnetized domain state has been determined, the differences in magnetization reversal of single and multi domain dots may be discussed. Interestingly, no difference in the shape of the perpendicular hysteresis curves can be found. However, when comparing only the single domain dot samples (*D* ranging from 60-80 nm), it shows that with decreasing dot size the coercivity increases. This phenomenon is in agreement with common single domain theory. The ratio between coercivity and effective anisotropy field is approximately 0.20. The dominant mechanism of magnetization reversal probably is some sort of incoherent rotation like curling.
The observation that there is no correlation between dot size and coercivity for the multi domain dot samples might indicate that the switching field more strongly depends on the roughness of the dot edges or the sharpness of the dot corners. Surprising result is that H_c of the SD dots is considerably smaller than H_c of the MD dots. This contradiction might be explained by a comparison of $H_{K,eff}$ between all samples. Therefore $H_{K,eff}$ was calculated from the ratio of the torque maximum and the magnetic moment and is also given in Table 3. Indeed, compared to the MD dots, a significantly lower effective anisotropy field is found for the SD dots. Note that for the SD dots $H_{K,eff}$

is approximately equal to the saturation field of the in-plane hysteresis curve (Figure 7). The variation in effective anisotropy field needs further understanding. Compared to the unpatterned $Co_{50}Ni_{50}$/Pt multilayer, $H_{K,eff}$ of the MD dots is about 50 % larger. The origin was found to be an increase in K_{eff}. Such an increase may be induced by the patterning process.

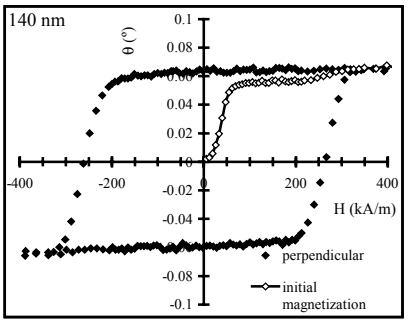

Figure 8: *Polar Kerr hysteresis and initial magnetization curves for 140/570 nm $Co_{50}Ni_{50}$/Pt multilayer dots.*

However, at these aspect ratios, shape effects can play an important role as well. The contribution of the shape anisotropy to this increase can be estimated roughly by approximating the dot shape with an oblate ellipsoid. With the analytical expression for the demagnetizing factor [86] and the proper expression for the shape anisotropy of a multilayer based on the mean square magnetization [87], it can be calculated that for 140 - 280 nm dots the shape anisotropy induces a 64 - 36 % increase of K_{eff}. Apparently, for the 140 - 280 nm dots the increase of $H_{K,eff}$ can also fully be explained from the reduced dimensions. The same increase should then be expected for the 60-80 nm dots. Since this is not the case, the intrinsic anisotropy of the multilayer itself must have been reduced. The most probable cause is the fact that these dots have partially been etched (see Figure 5). This observation has two consequences for the intrinsic perpendicular magnetic anisotropy. Firstly, the multilayer structure may be damaged. Most likely, a few bilayers in the upper part of the multilayer stack have been intermixed, which has destroyed the origin of the perpendicular anisotropy in these multilayers, i.e. interface anisotropy. Secondly, from other studies it is known that the lower part of as deposited $Co_{50}Ni_{50}$/Pt multilayers has lower perpendicular anisotropy than the upper part. Since the dot height has been reduced from 30 nm to approximately 15 nm and the dot has a pyramidal shape instead of a disk shape, the average perpendicular anisotropy will have been decreased. Concluding, it is likely that the origin of the smaller H_c of the SD dots is the reduction of intrinsic anisotropy.

5.3. ACTIVATION VOLUME AND THERMAL STABILITY OF SINGLE DOMAIN DOTS

The thermal stability of the 70 nm single domain dots has been investigated. In order to obtain an accurate value for the activation volume and relaxation time, both the hysteresis and the thermally activated switching at room temperature have been

measured by a Polar Kerr Magnetometer/Spectrometer (see eg [88]). Moreover, for the time dependent measurements the standard measurement procedure was adapted at two important points. Firstly, the data in the first 30 seconds was stored in the buffers of the lock-in amplifier to allow measurement on a short time scale. Figure 9 shows the measurements of hysteresis and magnetic viscosity. The activation volume at H_c has been calculated by using the equation (7) given in [104] and equals $(8 \pm 1) \times 10^{-18}$ cm^3, which is about six times smaller than the dot volume.

$$V_{act} = \frac{k_B T}{\mu_0 M_S} \cdot \frac{\chi_{irr}}{S} \qquad (7)$$

Where χ_{irr} is the irreversible susceptibility, which equals the derivative of the hysteresis curve if all reversal processes are irreversible; and S is the magnetic viscosity and is determined from the thermally activated switching of magnetization at a certain applied field.

The measured activation volume might be related to a volume of reduced magnetic anisotropy caused by etching damage induced in the patterning process. Since both the switching field distribution and the magnetic viscosity are roughly symmetric around H_C the activation volume can be assumed to be independent of the applied field.

The worst relaxation time τ_{min} (see formulae (10)) present in the sample corresponds to dots with H_C = 80 kA/m has been calculated to be 3.8×10^3 year by using the expression given in [105]. This value seems sufficient for storage. However, with statistical rules it can be calculated that in a 50 Gbit hard disk consisting of this type of dots already within 2.5 s a dot will have been switched by thermal activation. The reversal of a single dots in discrete media means complete data-loss, which is not the case in conventional media where reversal of a single grain does not necessarily mean that the data cannot be retrieved. Therefore the demand on thermal stability are more stringent for discrete media. Since the relaxation time is a steep function of the coercivity, a 50% increase in coercivity would solve the problem of thermally activated switching. It can be expected that by avoiding the etching damage of the 70 nm dots this can easily be achieved.

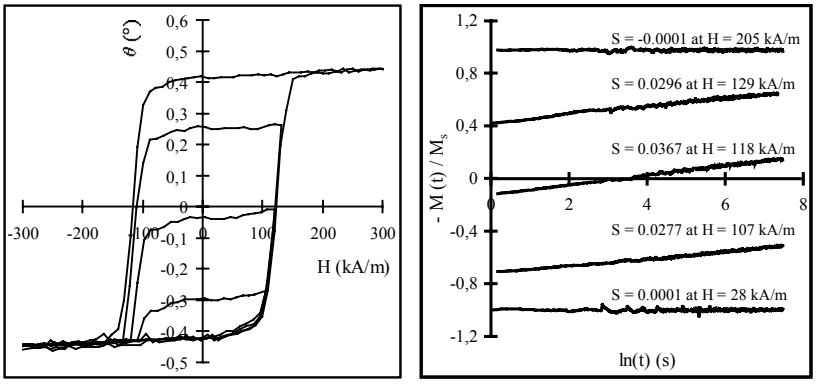

Figure 9: *Hysteresis and magnetic viscosity curves of single domain 70 nm $Co_{50}Ni_{50}$/Pt multilayer dots (measured with Polar Kerr Magnetometry at 570 nm).*

5.4. MAGNETIZATION REVERSAL

In section 4.1 the anisotropy field was calculated for several materials (see Table 2.). This was mentioned to be an upper limit of the switching field. To be more precise, this limit only applies in the absence of demagnetizing effects (or after correction for this). In this section the magnetization reversal of more practical shapes will be calculated and discussed.

5.4.1 Analytical calculations of magnetization reversal

In theoretical works the nucleation field H_N is defined as the (reverse) field where the magnetic state *starts* to deviate from uniform saturation (see e.g. [84]). Since only ellipsoids can exhibit a uniform magnetic state (and besides have a uniform demagnetizing field), the analytical calculations of the nucleation field are limited to this class of particles. Despite of this precondition, it is very instructive to use approximations by ellipsoids to calculate nucleation fields for other shapes. This provides insight in the relation between the nucleation field and the intrinsic material properties as saturation magnetization M_s, uniaxial anisotropy K_u and exchange constant A. It should be emphasized that in principle no estimation is made of the more relevant coercive field H_C, defined as the field where the average magnetization equals zero. Since H_C is by definition always larger (or more negative) than H_N, only a lower limit of H_C is calculated. For the case of a configuration with the applied field parallel to the easy axis of magnetization, two relevant modes of magnetization reversal exist which are the two analytical solutions of Brown's magnetostatic equations (see the original work by Brown [89] or the recent book by Aharoni [84]). These have been named coherent rotation and magnetization curling. The former one is valid for any ellipsoid, while the latter one is only valid for an ellipsoid of revolution, either prolate or oblate. The equations of the nucleation field of both modes are given and used to estimate the nucleation field of cylindrical $Co_{50}Ni_{50}$/Pt multilayer dots in [9]. The nucleation field can be written as in the useful form with reduced units:

$$H_N = 1 - \frac{N_z}{Q} \qquad [\mathrm{H_{K,\,u}}] \tag{8}$$

with Q as defined in Equation (5) and H_N in units of the anisotropy field. For $N_z = 1$ the lower limit of the nucleation field (thin film limit) is found. Since nucleation takes place by the mode with the lowest H_N, the transition from coherent to curling is found for (inhomogeneous) multilayers,

$$d_{curling} >> 2q\sqrt{\frac{2\overline{A}}{\mu_0\,\overline{M_s^2}}} \tag{9}$$

Here q is the factor depending on the size and shape of the particle and given by [84]:
q = 1.8412 for an infinitely long cylinder
q = 2.0816 for a sphere
q = 2.115 for an infinite plate.

This limit equals 500 kA/m for $Co_{50}Ni_{50}$/Pt multilayers and is valid for d >> 13 nm (and d>>h).

5.4.2. Micromagnetic calculations of magnetization reversal

Magnetic imaging and micromagnetic simulations have shown that nonuniform magnetization configuration in patterned structures can considerably effect the magnetization reversal (90,91). The mode of reversal determines directly the energy barrier that has to be overcome for switching. This barrier should be a high as possible, so that very small dots will still be thermally stable. For micromagnetic investigations of the magnetization reversal and to determine the single domain limit we use an existing 3Dimensional-micromagnetic-simulation package [92] using reduced units [93]. This is a straightforward extension of the one described in [94] to three-dimensions. Due the constraints imposed by the FFT method used for stray field computation, a uniform grid and rectangular computational areas are needed. The simulations are described in [95]. From the experimental data we know that the dots were not perfect cylinders due to etching damage but appear as truncated cones. From the magnetic studies we also know that the switching field H_{sw} is approximately 120 kA/m (H_{sw}/H_k = 0.08). The magnetization reversal does not show a sharp switching behavior. This is believed to be due to the inhomogeniety in the dot size and shape that would cause a widened switching distribution. We cannot incorporate all the experimental properties into the modeling but rather we use dots that are homogenous in size and shape. The multilayer structure of the dots is ignored and properties are average over the dot volume. The magnetic parameters used in the modeling are the uniaxial anisotropy constant K_u=480 kJ/m^3, exchange constant A= 3.10^{-12} J/m, saturation magnetization M_s=713 kA/m and the anisotropy field H_k = 1500 kA/m. The total energy (exchange, uniaxial anisotropy, stray field and external field) is minimized to find the equilibrium magnetization [96,97].

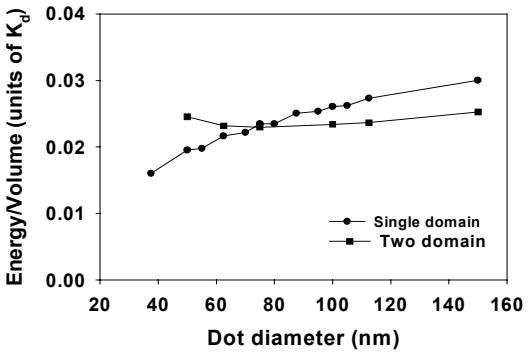

Figure 10. Energy of single amd two domain state of CoNi/Pt multilayer dots with at thickness h=30nm

Figure 10 shows the calculated total energy/unit volume of the single and two-domain state as a function of diameter in dots with a thickness of 30nm. The two curves intersect at about 75 nm. At this diameter, which we call the critical diameter, the

energy of both states is equal. The single domain state is the lowest energy state in dots with diameters below the critical diameter. Above the critical diameter it is energetically more favorable to divide the magnetization into two oppositely magnetized domains in order to reduce stray field energy, even though this is at the cost of creation of additional domain wall energy (exchange and anisotropy energy). MFM and VSM measurements show that 70nm dots are single domain and 180nm dots are multidomain (see figure 6 and 7), which is in agreement with the simulation. It should be noted however that we have not calculated the energy barrier between the single and two-domain state. It is very likely that both states are stable in a wide range of diameters, even at room temperature. Next to the total energy, the magnetization as a function of external field was simulated for different dot shapes (cylindrical, pointed cone and truncated cone) [95]. These simulations clearly show that the shape of the dots strongly influences the switching field, with values ranging from to 0.5 down to 0.22 H_k. To estimate the influence of etch damage, a soft-outer shell was implemented with thickness of 15% of the dot diameter. The simulated hysteresis curve for this truncated cone shaped dot (70 nm in diameter and 30 nm height), after the addition of the soft layers is given in Figure 11. The addition of the soft layers was found to reduce the value of H_{sw}/H_k from 0.22 down to 0.13, close to the experimental value of 0.08.
A critical remark should however be made with respect to the simulations. In all calculations the highly inhomogeneous $Co_{50}Ni_{50}$/Pt multilayers have been modeled as homogeneous material with averaged properties. Though the averaging was done in a careful way, the resulting uncertainty in the calculated switching field is hard to estimate. Moreover all simulations are performed at 0K: the switching field at room temperature will be lower, especially for these small structures.

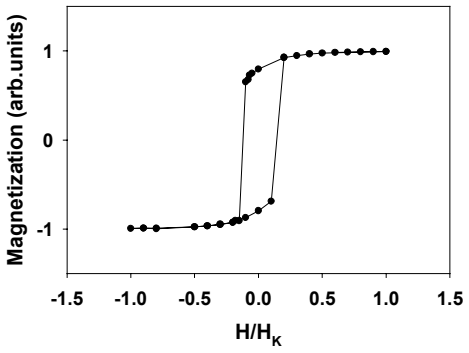

Figure 11. Magnetization Reversal of CoNi/Pt multilayer truncated cone shaped dot with a soft layer in the circumference

5.4.3. Magnetostatic interactions

The switching field distribution associated with the dipolar interaction between magnetic particles is proportional to the magnetization of the material. This interaction is strongly dependent on inter-particle distance, particle shape and saturation

magnetization. Therefore, a simple generalized expression for its magnitude cannot be given. Moreover, in the end the allowed switching field distribution will have to be defined by the tolerances of the storage device. Here, with respect to magnetostatic interactions only a firm statement can be made concerning the stability of the saturated state of a patterned medium. In zero field, the stability of the medium is not dependent on inter-particle distance and saturation magnetization if the uniaxial anisotropy is larger than the thin film shape anisotropy, i.e. if $Q > 1$ (Equation 5). This means that the highest bit/dot density can be obtained for materials with $Q > 1$. Table 4 shows the Q values of the materials discussed in section 4.1. It can be seen that these materials have a wide variety of Q values. From the point of view of bit density, single-element patterned media are clearly not suitable for storage purposes. Moreover, it will be difficult to obtain the intrinsic switching field distribution of densely packed single-element pillars.

TABLE 4: Q values (Equation 5) of several materials with uniaxial magnetic anisotropy (with Table 2).

Material	Q
Co (hcp)	0.34
Co (fcc)	(0.50) [1]
Ni	(0.50) [1]
Fe	(0.50) [1]
$BaFe_{12}O_{19}$	3.7
FePt ($L1_0$ phase)	5.2
TbFeCo	16
$Co_{50}Ni_{50}$/Pt (multilayer)	1.5

[1] For shape anisotropy of a quasi-infinitely elongated prism or cylinder.

6. Conclusions and outlook

6.1. LIL TECHNOLOGY

For the smallest dimensions of the dots considered here, the process latitude is limited. With a higher contrast resist, in combination with an antireflective coating, considerable improvement is achieved. Further progress may be limited by instabilities of the present exposure setup. At present the minimum period of the interference pattern is 200 nm. For a further decrease of feature dimensions the wavelength of the laser should be decreased. Recently, Hinsberg *et al.* showed interference lithography with a laser wavelength of 257 nm and the application of deep UV resists with high contrast [100]. Lasers with even smaller wavelength have poor temporal and spatial coherence and are therefore not suitable for laser interference lithography. However, achromatic interference lithography with ArF excimer lasers at 193 nm has the capability of patterning resist structures with periods of 100 nm [101,102]. The principle of the technique is the use of an exposure setup with vanishingly small difference in the length of the two light paths. Yen *et al.* proposed that this technique can be expanded for the patterning of structures with 50 nm period [103].

6.2 THE MATERIALS

At present the problem of thermal instability of written bits is a big issue in conventional magnetic recording. The relaxation time τ, which, in its most idealized form and assuming a prefactor of 10^{-10}, is given by [105]:

$$\tau = 10^{-10} \cdot e^{\frac{\frac{1}{2}\mu_0 M_S H_C V_{act}}{k_B T}} \qquad (10)$$

where: k_B = Boltzmann's constant, M_s = Saturation magnetisation, H_c = Coercivity, V_{act} = activation volume and T = temperature. For long-term storage purposes thermal relaxation should be prevented for sufficiently long time. Table 5 gives the minimum size of a cubic dot below which it becomes thermal unstable. All four materials (bariumferrite, Co or Fe based alloys with $L1_0$ phase, amorphous rare earth – transition metal alloys and Co based multilayers) have a large intrinsic uniaxial magnetic anisotropy, which guarantees a sufficiently large switching field and a long-term thermal stability.

TABLE 5: The size of a cubic element (lsp) at which the thermal relaxation time equals 10 years, for several materials with uniaxial magnetic anisotropy.

Material	**l_{sp} (nm)**
Co (hcp)	7
Co (fcc)	(4) [1]
Ni	(6) [1]
Fe	(3) [1]
$BaFe_{12}O_{19}$	8
FePt ($L1_0$ phase)	4
TbFeCo	12
$Co_{50}Ni_{50}$/Pt (multilayer)	7

[1] For prisms with dimensions l_{sp} x l_{sp} x $10l_{sp}$.

Moreover, the dots of the patterned medium can be shaped in such a way that magnetostatic interactions are suppressed. In this respect, single-element Co, Ni or Fe patterned media are disadvantageous because they suffer from too large magnetostatic interactions in a densely packed 2D dot-array and therefore will limit the ultimate bit density.

6.3. APPLICATION IN PROBE RECORDING SYSTEM

The effect of superparamagnetic behaviour will force industry to look for alternatives to the current hard disk technology media in the near future. If the current annual volume growth rate of 60% continues, these new technologies should enter the market 10-15 years from now. Discrete magnetic recording is seen by the major hard disk manufacturers as a possible next step in magnetic recording. These discrete magnetic media will most likely be on rotating disc systems, so circular patterns are required.

Although the square arrays produced by LIL are not directly suitable for application in disc systems, the results of the research on these arrays will be directly applicable. The only method known up to know to produce circular patterns of dots on disc is by means of e-beam lithography. The big advantage of LIL over e-beam lithography is the very low cost and high speed. So the LIL-method will certainly play a big role in the research on circular patterned media. Since the capacity of recording system and the data transfer are more or less proportional, next to an increase in density also an increase in data rate must be realised. This will cause the next "revolution" in hard disk technology: the increasing rotating speeds of the disc and the TByte/s data-rates through the single read/write head will again force the recording industry to look for alternatives. Scanning probe technology with arrays of read/write heads could be such an alternative [108-110]. The rectangular arrays produced by LIL are very suitable for scanning probe types of recording systems, and the Laser Interference Lithography technique could become a major production technique, provided that the periodicity of the structures is reduced to at least 50 nm. There are of course alternatives to discrete magnetic recording. One alternative is to avoid superparamagnetic behaviour of very small written bits by using media with very high anisotropy. The write fields which can be generated by conventional hard-disc heads will than be too low, and at the moment it does not seem likely that head materials with considerably higher saturation magnetisation will be found**.** The solution is to locally heat the medium in order to reduce the coercivity. This technique can of course also be applied to discrete media.

Acknowledgements

The authors are thankful to dr.S. Sindhu who worked out all the micromagnetic simulations, The Dutch Foundation for Fundamental Research on Matter (FOM), Royal Netherlands Academy of Arts and Sciences (KNAW) and Dutch Technology Foundation (STW) for financial assistance.

References

[1] www.storage.ibm.com/storage/technology/grochows/

[2] White R L, R.M.W.New and R.F.W.Pease (1997),Patterned media:A visable route to 50 Gbit/in^2 and up for magnetic recording, IEEE Trans.Magn.,33, 990-995

[3]. Todorovic M, S. Schultz , J Wong and A Scherer (1997)……, Appl.Phys.Lett, 74, 17, 2516-2518

[4]. Chappert C, H.Bernas, J.Ferre, V.Kottler, J-P Jamet, Y.Chen, E.Cambtil, T.Devolder, F.Rousseaux, V.Mathet andH.Launois (1998), Planar patterende magnetic media obtained by ion irradiotion, Science, 280, 1919-1922

[5] Chou, S.Y., P.R.Krauss (1996) Quantum magnetic disk J.Magn.Magn.Mater.155, 151-153

[6]. Rousseaux F, D. Decanini, F. Carcenac, E. Cambril, M.F. Ravet, C. Chappert, N. Bardou, B. Bartenlian, and P. Veillet, (1995) 'Study of large area high density magnetic dot arrays fabricated using synchotron radiation based x-ray lithography', J. Vac. Sci. Technol. B 13 2787-2791.

[7]. Ross, C.A., H.I.Smith, T.Savas, M.Schattenburg, M.Farhoud, M.Hwang, M.Walsh, M.C.Abraham, R.J. Ram (1999), *Fabrication of Patterned media for high density magnetic storage*, J.Vac.Sci.Technol.B, 6, 3168-3176

[8]. Axel A. Carl, S. Kirsch, J. Lohau, H. Weinforth and E.F. Wassermann, *Magnetization Reversal of Nanostructured Co/Pt Multilayer Dots and Films studied with Magnetic Force Microscopy and Moke"* , IEEE Trans. Magn. (1999)

[9]. Haast,M, (1999), Patterned magnetic thin films for ultra high density recording, PhD Thesis, University of Twente, Enschede, The Netherlands

[10]. Brown.M (1999), The growing disparity between magnetic density improvement and individual disk drive performance. Abstracts 44th Annual Conference on Magnetism and Magnetic Materials, page 330.

[11]. Vettiger P, J. Brugger, M. Despont, U. Drechsler, U. Durig, W. Haberle, M. Lutwyche, H. Rothuizen, R. Stutz, R. Widmer, and G. Binnig. (1999) Ultrahigh density, high-data-rate nems-based afm data storage system. Microelectronic Engineering, 46:1-4

[12]. L.F. Shew, IEEE Trans. Broad. Tel. Rec. 9 (1963) 56.

[13]. R.L. White, R.M.H. New, and R.F.W. Pease, *'Patterned media: a viable route to 50 Gbit/in^2 and up for magnetic recording'*,IEEE. Trans. Magn. 33 (1997) 990-995.

[14]. S.Y. Chou, *'Patterned magnetic nanostructures and quantized magnetic disks'*, Proc. IEEE 85 (1997) 652-671.

[15] M. Rothschild, J.A. Burns, S.G. Cann, A.R. Forte, C.L. Keast, R.R. Kunz, S.C. Palmateer, J.H.C. Sedlacek, R. Uttaro, A. Grenville, and D. Corliss, *'How practical is 193 nm lithography'*, J. Vac. Sci. Technol. B 14 (1996) 4157-4161.

[16] SEMATECH, ' *'The National Technology Roadmap for Semiconductors'* (1997).

[17] J.P. Silverman, *'Challenges and progress in x-ray lithography'*, J. Vac. Sci. Technol. B 16 (1998) 3137-3141.

[18] C.W. Gwyn, R. Stulen, D. Sweeney, and D. Attwood, *'Extreme ultraviolet lithography'*, J. Vac. Sci. Technol. B 16 (1998) 3142-3149.

[19] S.T. Stanton, J.A. Liddle, W.K. Waskiewicz, and A.E. Novembre, *'Critical dimension control at stitched subfield boundaries in a high-throughput SCALPEL® system'*, J. Vac. Sci. Technol. B 16 (1998) 3197-3201.

[20] G. Gross, R. Kaesmaier, H. Löschner, and G. Stengl, *'Ion projection lithography: Status of the MEDEA project and United States/European cooperation'*, J. Vac. Sci. Technol. B 16 (1998) 3150-3153.

[21] F. Rousseaux, D. Decanini, F. Carcenac, E. Cambril, M.F. Ravet, C. Chappert, N. Bardou, B. Bartenlian, and P. Veillet, *'Study of large area high density magnetic dot arrays fabricated using synchotron radiation based x-ray lithography'*, J. Vac. Sci. Technol. B 13 (1995) 2787-2791.

[22] H. Schmid, H. Biebuyck, B. Michel, O.J.F. Martin, and N.B. Piller, *'Light-coupling masks: An alternative, lensless approach to high-resolution optical contact lithography'*, J. Vac. Sci. Technol. B 16 (1998) 3422-3425.

[23] M.M. Alkaisi, R.J. Blaikie, and S.J. McNab, *'Nanolithography using wet etched silicon nitride phase masks'*, J. Vac. Sci. Technol. B 16 (1998) 3929-3933.

[24] R.J. Blaikie, M.M. Alkaisi, S.J. McNab, D.R.S. Cumming, R. Cheung, and D.G. Hasko, *'Nanolithography using optical contact exposure in the evanescent near field'*, Microelectronic Engineering, in press.

[25] S.Y. Chou, P.R. Krauss, and L. Kong, *'Nanolithographically defined magnetic structures and quantum magnetic disk'*, J. Appl. Phys. 79 (1996) 6101-6106.

[26] R.W. Jaszweski, H. Schift, J. Gobrecht, and P. Smith, *'Hot embossing in polymers as a direct way to pattern resist'*, Microelectronic Engineering 41/42 (1998) 575-578.

[27] X.M. Zhao, Y. Xia, and G.M. Whitesides, *'Soft lithographic methods for nano-fabrication'*, J. Mater. Chem. 7 (1997) 1069-1074.

[28] L. Kong, L. Zhuang, M. Li, B. Cui, and S.Y. Chou, *'Fabrication, writing and reading of 10 Gbits-in^2 longitudinal quantized magnetic disks with a switching field over 1000 Oe'*, Jpn. J. Appl. Phys. 37 (1998) 5973-5975.

[29] H.C. Scheer, H. Schulz, T. Hoffmann, and C.M. Sotomayor Torres, *'Problems of the nanoimprinting technique for nanometer scale pattern definition'*, J. Vac. Sci. Technol. B 16 (1998) 3917-3921.

[30] H.A. Biebuyck, N.B. Larsen, E. Delamarche, and B. Michel, *'Lithography beyond light: Microcontact printing with monolayer resists'*, IBM J. Res. Develop. 41 (1997) 159-170.

[31] S. Zhu, R.J. Gambino, M.H. Rafailovich, J. Sokolov, S.A. Schwarz, and R.D. Gomez, *'Microscopic magnetic characterization of submicron cobalt islands prepared using self assembled polymer masking technique'*, IEEE Trans. Magn. 33 (1997) 3022-3024.

[32] R. Allenspach, A. Bischof, U. Dürig, and P. Grütter, *Local modification of magnetic properties by an electron beam'*, Appl. Phys. Lett. 73 (1998) 3598-3600.

[33] T. Aign, P. Meyer, S. Lemerle, J.P. Jamet, J. Ferré, V. Matthet, C. Chappert, J. Gierak, C. Vieu, F. Rousseaux, H. Launois, and H. Bernas, *'Magnetization reversal in arrays of perpendicularly magnetized ultrathin dots coupled by dipolar interaction'*, Phys. Rev. Lett. 81 (1998) 5656-5659.

[34] K. Bessho, Y. Iwasaki, and S. Hashimoto, *'Fabricating nanoscale magnetic mounds using a scanning probe microscope'*, J. Appl. Phys. 79 (1996) 5057-5059.

[35] J. Tersoff, C. Teichert, and M.G. Lagally, *'Self-organization in growth of quantum dot superlattices'*, Phys. Rev. Lett. 76 (1996) 1675-1678.

[36] C. Teichert, J. Barthel, H.P. Oepen, and J. Kirschner, *Fabrication of nanomagnet arrays by shadow deposition on self-organized semiconductor substrates'*, Appl. Phys. Lett. 74 (1999) 588-590.

[37] R.J. Celotta, R. Gupta, R.E. Scholten, and J.J. McCelland, *'Nanostructure fabrication via laser-focussed atomic deposition'*, J. Appl. Phys. 79 (1996) 6079-6083.

[38] W. Lu, K.G.H. Baldwin, M.D. Hoogerland, S.J. Buckman, T.J. Senden, T.E. Sheridan, and R.W. Boswell, *'Sharp edged silicon structures generated using atom lithography with metastable helium atoms'*, J. Vac. Sci. Technol. B 16 (1998) 3846-3849.

[39] J.H. Thywissen, K.S. Johnson, N.H. Dekker, A.P. Chu, and M. Prentiss, *'Using neutral atoms and standing light waves to form a calibration artifact for length metrology'*, J. Vac. Sci. Technol. B 16 (1998) 3841-3845.

[40] J. Fujita, T. Kisimoto, M. Morinaga, S. Matsui, and F. Shimizu, *'Atomic beam holography for nanofabrication'*, J. Vac. Sci. Technol. B 16 (1998) 3855-3858.

[41] O. Dial, C.C. Cheng, and A. Scherer, *'Fabrication of high-density nanostructures by electron beam lithography'*, J. Vac. Sci. Technol. B 16 (1998) 3887-3890.

[42] R.M.H. New, R.F.W. Pease, and R.L. White, *'Submicron patterning of thin cobalt films for magnetic storage'*, J. Vac. Sci. Technol. B 12 (1994) 3196-3201.

[43] P.R. Krauss, and S.Y. Chou, *'Fabrication of planar quantum magnetic disk structure using electron beam lithography, reactive ion etching and chemical mechanical polishing'*, J. Vac. Sci. Technol. B 13 (1998) 2850-2852.

[44] R. O'Barr, S.Y. Yamamoto, S. Schultz, W. Xu, and A. Scherer, *Fabrication and characterization of nanoscale arrays of nickel columns'*, J. Appl. Phys. 81 (1997) 4730-4732.

[45] L.F. Johnson, G.W. Kammlott, and K.A. Ingersoll, *'Generation of periodic surface corrugations'*, Applied Optics 17 (1978) 1165-1181.

[46] E.H. Anderson, C.M. Horwitz, and H.I. Smith, *'Holographic lithography with thick photoresist'*, Appl. Phys. Lett. 43 (1983) 874-875.

[47] J.P. Spallas, A.M. Hawryluk, and D.R. Kania, *'Field emitter array mask patterning using laser interference lithography'*, J. Vac. Sci. Technol. B 13 (1995) 1973-1978.

[48] X. Chen, S.H. Zaidi, S.R.J. Brueck, and D.J. Devine, *'Interferometric lithography of sub-micrometer sparse hole arrays for field-emission display applications'*, J. Vac. Sci. Technol. B 14 (1996) 3339-3349.

[49] J. Nole, *'Holographic lithography needs no mask'*, Laser Focus World (1997) 209-212.

[50] A. Fernandez, P.J. Bedrossian, S.L. Baker, S.P. Vernon, and D.R. Kania, *'Magnetic force microscopy of single-domain cobalt dots patterned using interference lithography'*, IEEE Trans. Magn. 32 (1996) 4472-4474.

[51] E.F. Wassermann, M. Thielen, S. Kirsch, A. Pollmann, H. Weinforth, and A. Carl, *'Fabrication of large scale periodic magnetic nanostructures'*, J. Appl. Phys. 83 (1998) 1753-1757.

[52] M. Farhoud, M. Hwang, H.I. Smith, M.L. Schattenburg, J.M. Bae, K. Youcef-Toumi, and C.A. Ross, *'Fabrication of large area nanostructured magnets by interferometric lithography'*, IEEE Trans. Magn. 34 (1998) 1087-1089.

[53] M.A.M. Haast, J.R. Schuurhuis, L. Abelmann, J.C. Lodder, and Th.J.A. Popma, *'Reversal mechanism of submicron patterned CoNi/Pt multilayer dots'*, IEEE Trans. Magn. 34 (1998) 1006-1008.

[54] D.H. Raguin, and G.M. Morris, *'Structured surfaces mimic coating performance'*, Laser Focus World (1997) 113-117.

[55] V. Berger, O. Gauthier-Lafaye, and E. Costard, *'Photonic band gaps and holography'*, J. Appl. Phys. 82 (1997) 60-64.

[56] C.J.M. van Rijn, G.J. Veldhuis, and S. Kuiper, *'Nanosieves with microsystem technology for microfiltration applications'*, Nanotechnology 9 (1998) 343-345.

[57] W. Wu, B. Cui, X.Y. Sun, W. Zhang, L. Zhuang, L. Kong, and S.Y. Chou, *'Large area high density quantized magnetic disks fabricated using nanoimprint lithography'*, J. Vac. Sci. Technol. B 16 (1998) 3825-3829.

[58] M.L. Schattenburg, C.R. Canizares, D. Dewey, K.A. Flanagan, A. Hammett, A.M. Levine, K.S.K. Lam, R. Manikkalingam, T. Markert, and H.I. Smith, *'Transmission grating spectroscopy and the Advanced X-ray Astrophysics Facility'*, Opt. Eng. 30 (1991) 1590-1600.

[59] J.P. Spallas, R.D. Boyd, J.A. Britten, A. Fernandez, A.M. Hawryluk, M.D. Perry, and D.R. Kania, *'Fabrication of sub-0.5 μm diameter cobalt dots on silicon substrates and photoresist pedestals on 50 cm x 50 cm glass substrates using laser interference lithography'*, J. Vac. Sci. Technol. B 14 (1996) 2005-2007.

[60] M.A.M. Haast, I.R. Heskamp, L. Abelmann, J.C. Lodder, and Th.J.A. Popma, *'Magnetic characterization of large area arrays of single and multi domain CoNi/Pt multilayer dots'*, J. Magn. Magn. Mat. 193 (1999) 511-514.

[61] A. Fernandez, H.T. Nguyen, J.A. Britten, R.D. Boyd, M.D. Perry, D.R. Kania, and A.M. Hawryluk, *'Use of interference lithography to pattern arrays of submicron resist structures for field emission flat panel displays'*, J. Vac. Sci. Technol. B 15 (1997) 729-735.

[62] A. Fernandez, J.Y. Decker, S.M. Herman, D.W. Phillion, D.W. Sweeney, and M.D. Perry, *'Methods for fabricating arrays of holes using interference lithography'*, J. Vac. Sci. Technol. B 15 (1997) 2439-2443.

[63] C. Chappert, H. Bernas, J. Ferré, V. Kottler, J.P. Jamet, Y. Chen, E. Cambril, T. Devolder, F. Rousseaux, V. Mathet, and H. Launois, *'Planar patterned magnetic media obtained by ion irradiation'*, Science 280 (1998) 1919-1922.

[64] P.F. Carcia, A.D. Meinhaldt, and A. Suna, *'Perpendicular magnetic anisotropy in Pd/Co thin film layered structures'*, Appl. Phys. Lett 47 (1985) 178-180.

[65] P.F. Carcia, *'Perpendicular magnetic anisotropy in Pd/Co and Pt/Co thin film layered structures'*, J. Appl. Phys. 63 (1988) 5066-5073.

[66] W.B. Zeper, H.W. van Kesteren, B.A.J. Jacobs, J.H.M. Spruit, and P.F. Carcia, *'Hysteresis, microstructure, and magneto-optical recording in Co/Pt and Co/Pd multilayers'*, J. Appl. Phys. 70 (1991) 2264-2271.

[67] S. Hashimoto, A. Maesaka, K. Fujimoto, and K. Bessho, '*Magneto-optical applications of Co/Pt multilayers'*, J. Magn. Magn. Mat. 121 (1993) 471-478.

[68] C.J. Lin, *'Co/Pt multilayers for magneto-optical recording'* in: *'High density digital recording'*, edited by K.H.J. Busschow and G.J. Long, Kluwer (1993) 461-481.

[69] P.F. Carcia, *'Evolution of metal multilayers for MO recording'*, J. Magn. Soc. Jpn. 19 S1 (1995) 5-16.

[70] M. Mes, J.C. Lodder, T. Takahata, I. Moritani, and N. Imamura, *'Evaporated CoNi/Pt multilayers for magneto-optical recording'*, J. Magn. Soc. Jpn. 15 S1 (1993) 44 -??? .

[71] S. Hashimoto, *'Adding elements to the Co layer in Co/Pt multilayers'*, J. Appl. Phys. 75 (1993) 438-441.

[72] R. Krishnan, H. Lassri, M. Seddat, M. Porte, and M. Tessier, *'Magnetic properties of $Co_x Ni_{1-x}$ /Pt multilayers'*, Appl. Phys. Lett. 64 (1994) 2312-2314.

[73] Q. Meng, W.P. van Drent, J.C. Lodder, and Th.J.A. Popma, *'Curie temperature dependence of magnetic properties of CoNi/Pt multilayer films'*, J. Magn. Magn. Mat. 156 (1996) 296-298.

[74] J.G. Ha, K. Kyuno, and R. Yamamoto, *'Perpendicular magnetic anisotropy and magneto-optical properties of $(Co_{1-x}Ni_x)$/Pd multilayers'*, IEEE Trans. Magn. 33 (1997) 1049-1051.

[75] W.P. van Drent, *'CoNi/Pt multilayers for magneto-optical recording'*, Ph.D. thesis, Universiteit Twente, The Netherlands (1995).

[76] C. Kooy and U. Enz, *'Experimental and theoretical study of the domain configuration in thin layers of $BaFe_{12}O_{19}$'*, Philips Res. Rep. 15 (1960) 7-29.

[77] M. Hehn, S. Padovani, K. Ounadjela, and J.P. Bucher, *'Nanoscale magnetic domain structures in epitaxial cobalt films'*, Phys. Rev. B 54 (1996) 3428-3433.

[78] A. Lisfi, J.C. Lodder, P. de Haan, M.A. Smithers, and F.J.G. Roesthuis, *'Barium Ferrite Films grown by laser ablation'*, IEEE Trans. Magn. 34 (1998) 1654-1656.

[79] M.R. Visokay, and R. Sinclair, *'Direct formation of ordered CoPt and FePt compound thin films by sputtering'*, Appl. Phys. Lett. 66 (1995) 1692-1694.

[80] J.U. Thiele, L. Folks, M.F. Toney, and D.K.Weller, *'Perpendicular magnetic anisotropy and magnetic domain structure in sputtered epitaxial FePt (001) $L1_0$ films'*, J. Appl. Phys. 84 (1998) 5686-5692.

[81] V. Gehanno, A. Marty, B. Gilles, and Y. Samson, *'Magnetic domains in epitaxial ordered FePd(001) thin films with perpendicular magnetic anisotropy'*, Phys. Rev. B 55 (1997) 12552-12555.

[82] M.T. Johnson, R. Jungblut, P.J. Kelly, and F.J.A. den Broeder, *'Perpendicular magnetic anisotropy of multilayers: recent insights'*, J. Magn. Magn. Mat. 148 (1995) 118-124.

[83] H.J.G. Draaisma, F.J.A. den Broeder, and W.J.M. de Jonge, *'Magnetic interface anisotropy in Pd/Co and Pd/Fe multilayers'*, J. Magn. Magn. Mat. 66 (1987) 351-355.

[84] A. Aharoni, *'Introduction to the theory of ferromagnetism'*, Oxford Science Publications (1996).

[85] M.Ruhrig, S.Porthun, J.C.Lodder, S.McVitie, l.j.Heyderman, A.B.Johnston, J.N.Chapman, *Electron beam fabrication and characterisation of high resolution magnetic force tips,* J.Appl.Phys. 79(6) (1966), 2913-2919.

[86] G. Bottoni, D. Candolfo, A.. Cecchetti, and F. Masoli, *'Analysis of the magnetization switching using the rotational hysteresis integral'*, J. Magn. Magn. Mater. 193 (1999) 329-331.

[87] I.S. Jacobs and F.E. Luborsky, *'Magnetic anisotropy and rotational hysteresis in elongated fine-particle magnets'*, J. Appl. Phys. 28 (1957) 467-473.

[88] W.P. van Drent, *'CoNi/Pt multilayers for magneto-optical recording'*, Ph.D. thesis, Universiteit Twente, The Netherlands (1995).

[89] W.F. Brown, *'Micromagnetics'*, Interscience, New York (1963).

[90] Y.F.Zheng, J-G. Zhu, '*Switching field variation in patterned submicron magnetic film elements',* J.Appl.Phys.81, (1997), 5471

[91] J.Shi, T.Zhu, M.Durlam, E.Chen, S.Tehrani, Y.F.Zheng, J -G.Zhu, *End domain states and magnetization reversal in submicron magnetic structures* IEEE Trans Magn. 34 (1998) 997

[92] K. Ramstock, J. J.M. Ruigrok, J.C. Lodder*, Switching behavior of small soft magnetic elements* Sensors And Actuators A-Physical. 81: (1-3) (2000) 359-362, (or visit www.ramstock.de.)

[93] D.V.Berkov, K.Ramstock, A. Hubert, *Solving micromagnetic problems-towards an optimal numerical method,* Phys.Stat.Sol (a). 137(1993)207-225.

[94] A.Hubert, R. Schaefer, *Magnetic Domains: the analysis of magnetic microstructures*, Springer-Verlag, Berlin, Heidelberg, New-York, 1998) p.396.

[95] S.Sindhu, M.A.M.Haast, K. Ramstöck, L. Abelmann and J.C.Lodder *Micromagnetic simulations of the domain structure and the magnetization reversal of $Co_{50}Ni_{50}$/Pt multilayer dots*, Submitted for publication in JMMM, 2000

[96] D.V.Berkov, K.Ramstock, T.Leibl, A.Hubert *Numerical micromagnetics in low-anisotropy materials,*IEEE Trans Mag. 29 (1993) 2548.

[97] M.E. Schabes, A.Aharoni, Magnetostatic interaction fields for a 3-dimensional array of ferromagnetic cubes,IEEE Trans Mag. 23 (1987) 3882.

[98] M.E.Schabes, H.N.Bertram, *Magnetization processes in ferromagnetic cubes*, J. Appl. Phys. 64 (1988) 1347.

[99] R. Mattheis, K. Ramstock, J.McCord*, Formation and annihilation of edge walls in thin-film permalloy strips*, IEEE Trans Mag. 33(5) (1997), 3993-3995.

[100] W. Hinsberg, F.A. Houle, J. Hoffnagle, M. Sanchez, G. Wallraff, M. Morrison, and S. Frank, *'Deep-ultraviolet interferometric lithography as a tool for assessment of chemically amplified photoresist performance'*, J. Vac. Sci. Technol. B 16 (1998) 3689-3694.

[101] T.A. Savas, S.N. Shah, M.L. Schattenburg, J.M. Carter, and H.I. Smith, *'Achromatic interferometric lithography for 100 –nm-period gratings'*, J. Vac. Sci. Technol. B **13** (1995) 2732-2735.

[102] A. Yen, E.H. Anderson, R.A. Ghanbari, M.L. Schattenburg, and H.I. Smith, *'Achromatic holographic configuration for 100-nm-period lithography'*, Applied Optics 31 (1992) 4540-4545.

[103] A. Yen, M.L. Schattenburg, and H.I. Smith, *'Proposed method for fabricating 50-nm-period gratings by achromatic holographic lithography'*, Applied Optics **31** (1992) 2972-2973.

[104] E.P. Wohlfarth, 'The coefficient of magnetic viscosity', J. Phys. F: Met. Phys. 14 (1984) L155-L159.

[105] J.C. Mallinson, 'The Foundations of Magnetic Recording', Academic Press Inc., San Diego (1993)

[106] M. Mansuripur, *'The physical principles of magneto-optical recording'*, Cambridge University Press (1995).

[107] A.A. Kusov, S.S. Jaswal, and Z.S. Shan, *'Shape anisotropy of magnetic multilayers'*, Phys. Rev. B 46 (1992) 3123-3124.

[108]. L. Richard Carley, James A. Bain, Gary K. Fedder, David W. Greve, David F. Guillou, Michael S. C. Lu, Tamal Mukherjee, Suresh Santhanam, Leon Abelmann, Seungook Min, *Single Chip Computers With MEMS-Based Magnetic Memory (invited)*, J. of Appl. Phys. vol 87 (2000) no 9, p6680-6685

[109] Leon Abelmann, Sakhar Khizroev, Dmitri Litvinov, Jiang-Gang Zhu, James A. Bain, Mark H. Kryder, Klaus Ramstock, Cock Lodder, *Micromagnetic simulation of an ultra-small single pole perpendicular write head.,* J. of Appl. Phys., vol 87 (2000) no 9 p6680-6685

[110]. Leon Abelmann, Jiang-Gang Zhu, James A. Bain, Klaus Ramstock, Cock Lodder, *Micromagnetic simulation of a flux guide for a read head with sub 100 nm resolution*, J of Appl Phys, vol 87 (2000) no 9 p6636-6638